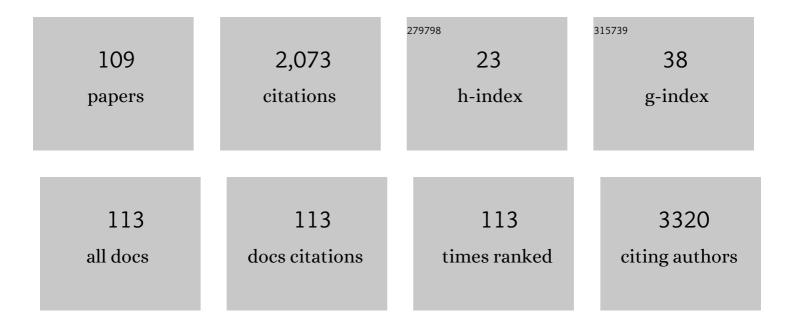
List of Publications by Year in descending order

Source: https://exaly.com/author-pdf/5965664/publications.pdf Version: 2024-02-01



#	Article	IF	CITATIONS
1	Predictive Value of Computed Tomography in Acute Pulmonary Embolism: Systematic Review and Meta-analysis. American Journal of Medicine, 2015, 128, 747-759.e2.	1.5	231
2	Subclinical Disease Burden as Assessed by Whole-Body MRI in Subjects With Prediabetes, Subjects With Diabetes, and Normal Control Subjects From the General Population: The KORA-MRI Study. Diabetes, 2017, 66, 158-169.	0.6	102
3	Hybrid cardiac imaging using PET/MRI: a joint position statement by the European Society of Cardiovascular Radiology (ESCR) and the European Association of Nuclear Medicine (EANM). European Radiology, 2018, 28, 4086-4101.	4.5	80
4	Automated reference-free detection of motion artifacts in magnetic resonance images. Magnetic Resonance Materials in Physics, Biology, and Medicine, 2018, 31, 243-256.	2.0	67
5	Computed tomography-based high-risk coronary plaque score to predict acute coronary syndrome among patients with acute chest pain – Results from the ROMICAT II trial. Journal of Cardiovascular Computed Tomography, 2015, 9, 538-545.	1.3	61
6	Validated imaging biomarkers as decision-making tools in clinical trials and routine practice: current status and recommendations from the EIBALL* subcommittee of the European Society of Radiology (ESR). Insights Into Imaging, 2019, 10, 87.	3.4	61
7	Glucose and insulin levels are associated with arterial stiffness and concentric remodeling of the heart. Cardiovascular Diabetology, 2019, 18, 145.	6.8	58
8	Cancer detection rates of the PI-RADSv2.1 assessment categories: systematic review and meta-analysis on lesion level and patient level. Prostate Cancer and Prostatic Diseases, 2022, 25, 256-263.	3.9	58
9	Incidence of Barotrauma in Patients With COVID-19 Pneumonia During Prolonged Invasive Mechanical Ventilation – A Case-Control Study. Journal of Intensive Care Medicine, 2021, 36, 477-483.	2.8	55
10	Pancreatic fat content by magnetic resonance imaging in subjects with prediabetes, diabetes, and controls from a general population without cardiovascular disease. PLoS ONE, 2017, 12, e0177154.	2.5	54
11	Feasibility of a three-step magnetic resonance imaging approach for the assessment of hepatic steatosis in an asymptomatic study population. European Radiology, 2016, 26, 1895-1904.	4.5	43
12	Impact of iterative metal artifact reduction on diagnostic image quality in patients with dental hardware. Acta Radiologica, 2017, 58, 279-285.	1.1	42
13	First Successful Treatment of Coronavirus Disease 2019 Induced Refractory Cardiogenic Plus Vasoplegic Shock by Combination of Percutaneous Ventricular Assist Device and Extracorporeal Membrane Oxygenation: A Case Report. ASAIO Journal, 2020, 66, 607-609.	1.6	37
14	Dynamic Myocardial Perfusion CT for the Detection of Hemodynamically Significant Coronary Artery Disease. JACC: Cardiovascular Imaging, 2022, 15, 75-87.	5.3	37
15	Renal and renal sinus fat volumes as quantified by magnetic resonance imaging in subjects with prediabetes, diabetes, and normal glucose tolerance. PLoS ONE, 2020, 15, e0216635.	2.5	36
16	Association of serum uric acid with visceral, subcutaneous and hepatic fat quantified by magnetic resonance imaging. Scientific Reports, 2020, 10, 442.	3.3	35
17	Coronary Computed Tomographic Angiography in Clinical Practice. Radiologic Clinics of North America, 2015, 53, 287-296.	1.8	32
18	Myocardial tissue characterization by contrast-enhanced cardiac magnetic resonance imaging in subjects with prediabetes, diabetes, and normal controls with preserved ejection fraction from the general population. European Heart Journal Cardiovascular Imaging, 2018, 19, 701-708.	1.2	31

#	Article	IF	CITATIONS
19	Pulmonary artery thrombi are co-located with opacifications in SARS-CoV2 induced ARDS. Respiratory Medicine, 2020, 172, 106135.	2.9	30
20	Dynamic CT myocardial perfusion imaging identifies early perfusion abnormalities in diabetes and hypertension: Insights from a multicenter registry. Journal of Cardiovascular Computed Tomography, 2016, 10, 301-308.	1.3	29
21	Are subpleural consolidations indicators for segmental pulmonary embolism in COVID-19?. Intensive Care Medicine, 2020, 46, 1109-1110.	8.2	29
22	The utility of multiparametric MRI to characterize hypoxic tumor subvolumes in comparison to FMISO PET/CT. Consequences for diagnosis and chemoradiation treatment planning in head and neck cancer. Radiotherapy and Oncology, 2020, 150, 128-135.	0.6	28
23	Long-term effect of physical inactivity on thoracic and lumbar disc degeneration—an MRI-based analysis of 385 individuals from the general population. Spine Journal, 2020, 20, 1386-1396.	1.3	25
24	Low-Volume Contrast Medium Protocol for Comprehensive Cardiac and Aortoiliac CT Assessment in the Context of Transcatheter Aortic Valve Replacement. Academic Radiology, 2015, 22, 1138-1146.	2.5	24
25	Predictive value of coronary computed tomography angiography in asymptomatic individuals with diabetes mellitus: Systematic review and meta-analysis. Journal of Cardiovascular Computed Tomography, 2018, 12, 320-328.	1.3	24
26	Clinical use of cardiac PET/MRI: current state-of-the-art and potential future applications. Japanese Journal of Radiology, 2018, 36, 313-323.	2.4	24
27	Clinical Significance of Intraluminal Contrast Enhancement in Patients with Spontaneous Cervical Artery Dissection: AÂBlack-Blood MRI Study. RoFo Fortschritte Auf Dem Gebiet Der Rontgenstrahlen Und Der Bildgebenden Verfahren, 2017, 189, 624-631.	1.3	23
28	Association between abdominal adiposity and subclinical measures of left-ventricular remodeling in diabetics, prediabetics and normal controls without history of cardiovascular disease as measured by magnetic resonance imaging: results from the KORA-FF4 Study. Cardiovascular Diabetology, 2018, 17, 88.	6.8	21
29	Artificial Intelligence in Magnetic Resonance Imaging–based Prostate Cancer Diagnosis: Where Do We Stand in 2021?. European Urology Focus, 2022, 8, 409-417.	3.1	21
30	Assessment of the degree of abdominal myosteatosis by magnetic resonance imaging in subjects with diabetes, prediabetes and healthy controls from the general population. European Journal of Radiology, 2018, 105, 261-268.	2.6	20
31	Feasibility of accelerated simultaneous multislice diffusionâ€weighted MRI of the prostate. Journal of Magnetic Resonance Imaging, 2017, 46, 1507-1515.	3.4	19
32	High-Sensitivity Cardiac Troponin I as a Gatekeeper for Coronary Computed Tomography Angiography and stress Testing in Patients with Acute Chest Pain. Clinical Chemistry, 2017, 63, 1724-1733.	3.2	19
33	Structured Reporting in Cross-Sectional Imaging of the Heart: Reporting Templates for CMR Imaging of Cardiomyopathies (Myocarditis, Dilated Cardiomyopathy, Hypertrophic Cardiomyopathy,) Tj ETQq1 1 0.784	314 rgBT /C	Overlock 10
34	Der Rontgenstrahlen Und Der Bildgebenden Verfahren. 2020. 192. 27-37. Bone marrow fat fraction assessment in regard to physical activity: KORA FF4–3-T MR imaging in a population-based cohort. European Radiology, 2020, 30, 3417-3428.	4.5	19
35	Chondrogenic Bone Tumors: The Importance of Imaging Characteristics. RoFo Fortschritte Auf Dem Gebiet Der Rontgenstrahlen Und Der Bildgebenden Verfahren, 2021, 193, 262-275.	1.3	19
36	Feasibility of CAIPIRINHA-Dixon-TWIST-VIBE for dynamic contrast-enhanced MRI of the prostate. European Journal of Radiology, 2015, 84, 2110-2116.	2.6	18

#	Article	IF	CITATIONS
37	Revised FIGO Staging for Cervical Cancer – A New Role for MRI. RoFo Fortschritte Auf Dem Gebiet Der Rontgenstrahlen Und Der Bildgebenden Verfahren, 2020, 192, 937-944.	1.3	18
38	Evaluation of reduced-dose CT for acute non-traumatic abdominal pain: evaluation of diagnostic accuracy in comparison to standard-dose CT. Acta Radiologica, 2018, 59, 4-12.	1,1	17
39	Quantitative 3-T Magnetic Resonance Imaging After Matrix-Associated Autologous Chondrocyte Implantation With Autologous Bone Grafting of the Knee: The Importance of Subchondral Bone Parameters. American Journal of Sports Medicine, 2021, 49, 476-486.	4.2	17
40	Highly sensitive troponin and coronary computed tomography angiography in the evaluation of suspected acute coronary syndrome in the emergency department. European Heart Journal, 2016, 37, 2397-2405.	2.2	16
41	Hepatic fat is superior to BMI, visceral and pancreatic fat as a potential risk biomarker for neurodegenerative disease. European Radiology, 2019, 29, 6662-6670.	4.5	16
42	Noise-optimized monoenergetic post-processing improves visualization of incidental pulmonary embolism in cancer patients undergoing single-pass dual-energy computed tomography. Radiologia Medica, 2017, 122, 280-287.	7.7	14
43	Inter- and intra-observer variability of an anatomical landmark-based, manual segmentation method by MRI for the assessment of skeletal muscle fat content and area in subjects from the general population. British Journal of Radiology, 2018, 91, 20180019.	2.2	14
44	Virtual non-enhanced dual-energy CT reconstruction may replace true non-enhanced CT scans in the setting of suspected active hemorrhage. European Journal of Radiology, 2018, 109, 218-222.	2.6	14
45	Distribution patterns of intramyocellular and extramyocellular fat by magnetic resonance imaging in subjects with diabetes, prediabetes and normoglycaemic controls. Diabetes, Obesity and Metabolism, 2021, 23, 1868-1878.	4.4	14
46	Morphologic performance analysis of the Relay nonbare stent graft in dissected thoracic aorta. Journal of Vascular Surgery, 2019, 70, 1390-1398.	1.1	13
47	An uncertainty-aware, shareable, and transparent neural network architecture for brain-age modeling. Science Advances, 2022, 8, eabg9471.	10.3	13
48	Spinal dual-energy computed tomography: improved visualisation of spinal tumorous growth with a noise-optimised advanced monoenergetic post-processing algorithm. Neuroradiology, 2016, 58, 1093-1102.	2.2	12
49	Evidencia cientÃfica reciente yÂavances técnicos en la tomografÃa computarizada cardiovascular. Revista Espanola De Cardiologia, 2016, 69, 509-514.	1.2	12
50	The evolution of radiation dose over time: Measurement of a patient cohort undergoing whole-body examinations on three computer tomography generations. European Journal of Radiology, 2017, 86, 63-69.	2.6	12
51	Cardiac Computed Tomography – More Than Coronary Arteries? AÂClinical Update. RoFo Fortschritte Auf Dem Gebiet Der Rontgenstrahlen Und Der Bildgebenden Verfahren, 2019, 191, 817-826.	1.3	12
52	Association of longitudinal risk profile trajectory clusters with adipose tissue depots measured by magnetic resonance imaging. Scientific Reports, 2019, 9, 16972.	3.3	12
53	PSMA-PET- and MRI-Based Focal Dose Escalated Radiation Therapy of Primary Prostate Cancer: Planned Safety Analysis of a Nonrandomized 2-Armed Phase 2 Trial (ARO2020-01). International Journal of Radiation Oncology Biology Physics, 2022, 113, 1025-1035.	0.8	12
54	Role of Imaging in Transcatheter Aortic Valve Replacement. Current Treatment Options in Cardiovascular Medicine, 2016, 18, 59.	0.9	11

#	Article	IF	CITATIONS
55	Selfâ€gated 4Dâ€MRI of the liver: Initial clinical results of continuous multiphase imaging of hepatic enhancement. Journal of Magnetic Resonance Imaging, 2018, 47, 459-467.	3.4	11
56	Age- and sex-based resource utilisation and costs in patients with acute chest pain undergoing cardiac CT angiography: pooled evidence from ROMICAT II and ACRIN-PA trials. European Radiology, 2018, 28, 851-860.	4.5	11
57	Population-based imaging biobanks as source of big data. Radiologia Medica, 2017, 122, 430-436.	7.7	10
58	Effect of reduced z-axis scan coverage on diagnostic performance and radiation dose of neck computed tomography in patients with suspected cervical abscess. PLoS ONE, 2017, 12, e0180671.	2.5	10
59	lsocaloric Substitution of Dietary Carbohydrate Intake with Fat Intake and MRI-Determined Total Volumes of Visceral, Subcutaneous and Hepatic Fat Content in Middle-Aged Adults. Nutrients, 2019, 11, 1151.	4.1	10
60	Characteristics and associated risk factors of diverticular disease assessed by magnetic resonance imaging in subjects from a Western general population. European Radiology, 2019, 29, 1094-1103.	4.5	10
61	Association of smoking and physical inactivity with MRI derived changes in cardiac function and structure in cardiovascular healthy subjects. Scientific Reports, 2019, 9, 18616.	3.3	9
62	MRI-Derived Radiomics Features of Hepatic Fat Predict Metabolic States in Individuals without Cardiovascular Disease. Academic Radiology, 2021, 28, S1-S10.	2.5	9
63	Stress myocardial perfusion with qualitative magnetic resonance and quantitative dynamic computed tomography: comparison of diagnostic performance and incremental value over coronary computed tomography angiography. European Heart Journal Cardiovascular Imaging, 2020, , .	1.2	9
64	Patellar instability MRI measurements are associated with knee joint degeneration after reconstruction of the medial patellofemoral ligament. Skeletal Radiology, 2022, 51, 535-547.	2.0	9
65	White matter hyperintensity volume in pre-diabetes, diabetes and normoglycemia. BMJ Open Diabetes Research and Care, 2021, 9, e002050.	2.8	8
66	The Lodwick classification for grading growth rate of lytic bone tumors: a decision tree approach. Skeletal Radiology, 2022, 51, 737-745.	2.0	8
67	Populationâ€based cohort imaging: skeletal muscle mass by magnetic resonance imaging in correlation to bioelectricalâ€impedance analysis. Journal of Cachexia, Sarcopenia and Muscle, 2022, 13, 976-986.	7.3	8
68	Quality and safety of coronary computed tomography angiography at academic and non-academic sites: insights from a large European registry (ESCR MR/CT Registry). European Radiology, 2022, 32, 5246-5255.	4.5	8
69	Recent Scientific Evidence and Technical Developments in Cardiovascular Computed Tomography. Revista Espanola De Cardiologia (English Ed), 2016, 69, 509-514.	0.6	7
70	Vertebral Bone Marrow Fat Is independently Associated to VAT but Not to SAT: KORA FF4—Whole-Body MR Imaging in a Population-Based Cohort. Nutrients, 2020, 12, 1527.	4.1	7
71	Management and endovascular therapy of ureteroarterial fistulas: experience from a single center and review of the literature. CVIR Endovascular, 2021, 4, 36.	1.1	7
72	Differences in coronary artery disease by CT angiography between patients developing unstable angina pectoris vs. major adverse cardiac events. European Journal of Radiology, 2014, 83, 1113-1119.	2.6	6

#	Article	IF	CITATIONS
73	Feasibility of free-breathing, GRAPPA-based, real-time cardiac cine assessment of left-ventricular function in cardiovascular patients at 3 T. European Journal of Radiology, 2015, 84, 849-855.	2.6	6
74	Impact of Radiation Dose Reduction in Abdominal Computed Tomography on Diagnostic Accuracy and Diagnostic Performance in Patients with Suspected Appendicitis. Academic Radiology, 2018, 25, 309-316.	2.5	6
75	Effects of Radiation Dose Reduction on Diagnostic Accuracy of Abdominal CT in Young Adults with Suspected Acute Diverticulitis: A Retrospective Intraindividual Analysis. Academic Radiology, 2019, 26, 782-790.	2.5	6
76	Association between Adipose Tissue Depots and Dyslipidemia: The KORA-MRI Population-Based Study. Nutrients, 2022, 14, 797.	4.1	6
77	Automated segmentation of head CT scans for computer-assisted craniomaxillofacial surgery applying a hierarchical patch-based stack of convolutional neural networks. International Journal of Computer Assisted Radiology and Surgery, 2022, 17, 2093-2101.	2.8	6
78	Automated MR-based lung volume segmentation in population-based whole-body MR imaging: correlation with clinical characteristics, pulmonary function testing and obstructive lung disease. European Radiology, 2019, 29, 1595-1606.	4.5	5
79	Impact of Preprocedural Aortic Valve Calcification on Conduction Disturbances after Transfemoral Aortic Valve Replacement. Cardiology, 2021, 146, 228-237.	1.4	5
80	Assessment of aortic annulus dimensions for transcatheter aortic valve replacement (TAVR) with high-pitch dual-source CT: Comparison of systolic high-pitch vs. multiphasic data acquisition. European Journal of Radiology, 2020, 133, 109366.	2.6	5
81	MRI phenotype of the prostate: Transition zone radiomics analysis improves explanation of prostate-specific antigen (PSA) serum level compared to volume measurement alone. European Journal of Radiology, 2020, 129, 109063.	2.6	5
82	Serum insulin is associated with right ventricle function parameters and lung volumes in subjects free of cardiovascular disease. European Journal of Endocrinology, 2021, 184, 289-298.	3.7	5
83	Subclinical cardiac impairment relates to traditional pulmonary function test parameters and lung volume as derived from whole-body MRI in a population-based cohort study. Scientific Reports, 2021, 11, 16173.	3.3	5
84	OUP accepted manuscript. Interactive Cardiovascular and Thoracic Surgery, 2021, , .	1.1	5
85	Genetic and clinical determinants of abdominal aortic diameter: genome-wide association studies, exome array data and Mendelian randomization study. Human Molecular Genetics, 2022, 31, 3566-3579.	2.9	5
86	Cardiac CT for Guiding Mitral Valve Interventions. Current Cardiovascular Imaging Reports, 2017, 10, 1.	0.6	4
87	Association of antecedent cardiovascular risk factor levels and trajectories with cardiovascular magnetic resonance-derived cardiac function and structure. Journal of Cardiovascular Magnetic Resonance, 2021, 23, 2.	3.3	4
88	Association of MRIâ€based adrenal gland volume and impaired glucose metabolism in a populationâ€based cohort study. Diabetes/Metabolism Research and Reviews, 2022, 38, e3528.	4.0	4
89	CoRad-19 – Modular Digital Teaching during the SARS-CoV-2 Pandemic. RoFo Fortschritte Auf Dem Gebiet Der Rontgenstrahlen Und Der Bildgebenden Verfahren, 2022, , .	1.3	4
90	Imaging-based characterization of cardiometabolic phenotypes focusing on whole-body MRl—an approach to disease prevention and personalized treatment. British Journal of Radiology, 2016, 89, 20150829.	2.2	3

FABIAN BAMBERG

#	Article	IF	CITATIONS
91	Quantitative Imaging and Imaging Biomarkers. Journal of Thoracic Imaging, 2018, 33, 69-70.	1.5	3
92	Machine-learning based exploration of determinants of gray matter volume in the KORA-MRI study. Scientific Reports, 2020, 10, 8363.	3.3	3
93	Incidental findings in whole-body MR imaging of a population-based cohort study: Frequency, management and psychosocial consequences. European Journal of Radiology, 2021, 134, 109451.	2.6	3
94	Significant Impact of Coffee Consumption on MR-Based Measures of Cardiac Function in a Population-Based Cohort Study without Manifest Cardiovascular Disease. Nutrients, 2021, 13, 1275.	4.1	3
95	The impact of transcatheter aortic valve implantation planning and procedure on acute and chronic renal failure. Cardiology Journal, 2021, , .	1.2	3
96	Association of Habitual Dietary Intake with Liver Iron—A Population-Based Imaging Study. Nutrients, 2022, 14, 132.	4.1	3
97	The Whole Is Greater Than the Sum ofÂitsÂParts. JACC: Cardiovascular Imaging, 2015, 8, 1282-1284.	5.3	2
98	Volumetric Surface-guided Graph-based Segmentation of Cardiac Adipose Tissues on Fat-Water MR Images. , 2019, , .		2
99	Spatial and Hierarchical Riemannian Dimensionality Reduction and Dictionary Learning for Segmenting Multichannel Images. , 2019, , .		2
100	More Than Detection of Adenocarcinoma – Indications and Findings in Prostate MRI in Benign Prostatic Disorders. RoFo Fortschritte Auf Dem Gebiet Der Rontgenstrahlen Und Der Bildgebenden Verfahren, 2022, , .	1.3	2
101	Distribution and Associated Factors of Hepatic Iron—A Population-Based Imaging Study. Metabolites, 2021, 11, 871.	2.9	2
102	Validity of fatty liver disease indices in the presence of alcohol consumption. Scandinavian Journal of Gastroenterology, 2022, 57, 1349-1360.	1.5	2
103	Case Report: Refusal of an Veno-Arterial Extracorporeal Membrane Oxygenation Due to Malignant Disease? — An Extremely Rare Form of Cardiac Involvement in Acute Myeloid Leukemia. Frontiers in Medicine, 2021, 8, 584507.	2.6	1
104	Evaluation of computed tomography settings in the context of visualization and discrimination of low dose injections of a novel liquid soft tissue fiducial marker in head and neck imaging. BMC Medical Imaging, 2021, 21, 157.	2.7	1
105	Whole-Body MRI-Derived Adipose Tissue Characterization and Relationship to Pulmonary Function Impairment. Tomography, 2022, 8, 560-569.	1.8	1
106	A combined partial volume reduction and super-resolution reconstruction for magnetic resonance images. , 2016, , .		0
107	Association between dietary fat intake and MRI-determined visceral, subcutaneous, or hepatic fat in men and women from the general population. Proceedings of the Nutrition Society, 2020, 79, .	1.0	Ο
108	Predicting Biochemical Failure in Irradiated Patients With Prostate Cancer by Tumour Volume Measured by Multiparametric MRI. In Vivo, 2020, 34, 3473-3481.	1.3	0

#	Article	IF	CITATIONS
109	Quantitative 3-T MRI Outcome Evaluation after Spongiosa-augmented MACI at the Knee: The Importance of Subchondral Bone Parameters. Seminars in Musculoskeletal Radiology, 2020, 24, .	0.7	0